CONTINUOUS PHASE MODULATION WITH FASTER-THAN-NYQUIST SIGNALING FOR CHANNELS WITH 1-BIT QUANTIZATION AND OVERSAMPLING AT THE RECEIVER

Rodrigo R. M. de Alencar and Lukas T. N. Landau

Centre for Telecommunications Studies
Pontifical Catholic University of Rio de Janeiro, Rio de Janeiro, Brazil 22453-900
Email: alencar;lukas.landau@cetuc.puc-rio.br

ABSTRACT

Continuous phase modulation (CPM) with 1-bit quantization at the receiver is promising in terms of energy and spectral efficiency. In this study, CPM waveforms with symbol durations significantly shorter than the inverse of the signal bandwidth are proposed, termed faster-than-Nyquist CPM. This configuration provides a better steering of zero-crossings as compared to conventional CPM. Numerical results confirm a superior performance in terms of BER in comparison with state-of-the-art methods, while having the same spectral efficiency and a lower oversampling factor. Moreover, the new waveform can be detected with low-complexity, which yields almost the same performance as using the BCJR algorithm.

Index Terms— 1-bit quantization, oversampling, continuous phase modulation, faster-than-Nyquist signaling.

1. INTRODUCTION

Continuous phase modulation (CPM) yields spectral efficiency, smooth phase transitions and a constant envelope [1, 2], which allows for the use of energy efficient power amplifiers with low dynamic range. At the receiver side, the energy consumption of the analog-to-digital converter (ADC) scales exponentially with the resolution in amplitude [3]. Hence, in this study a low resolution ADC is considered, where the ADC provides only sign information about the received signal. In order to compensate for the loss in terms of the achievable rate, oversampling with respect to (w.r.t.) the signal bandwidth is considered. In this context, it is shown that oversampling yields a significant gain in terms of achievable rate for the noiseless [4] and for the noisy channel [5].

As the information is implicitly conveyed in phase transitions of CPM signals, resolution in time is more promising than resolution of amplitude. CPM signals with channels with 1-bit quantization and oversampling has been considered before in [6], where the achievable rate is studied and maximized via optimization of sequences. Later, more practical approaches were proposed in [7], where the intermediate frequency and the waveform is considered in a geometrical analysis of the phase transitions. Moreover, in [8] iterative detection and decoding is studied for CPM signals with 1-bit quantization and oversampling.

In the present study, a CPM waveform is introduced with a symbol duration that is only a fraction of the symbol duration of an equivalent CPFSK, which is promising in terms of construction of zero-crossings. The proposed CPM waveform conveys the same information per time interval as the common CPFSK while its bandwidth can be the same and even lower. Referring to the high signaling rate, like it is typical for *faster-than-Nyquist* signaling [9],

the novel waveform is termed faster-than-Nyquist continuous phase modulation (FTN-CPM). Numerical results confirm that the proposed waveform yields a significantly reduced bit error rate (BER) as compared to the existing methods [6, 7] with at least the same spectral efficiency. In addition, FTN-CPM can be detected with low-complexity and with a lower effective oversampling factor in comparison with the state-of-the-art methods.

The sequel is organized as follows: Section 2 defines the system model, whereas Section 3 describes the proposed waveform. Section 4 details the detection, including a proposed low-complexity method. Section 5 discusses numerical results, while Section VI shows the conclusions.

Sequences of scalars and vectors are denoted with $x^n = [x_1, \ldots, x_n]^T$ and $\boldsymbol{y}^n = [\boldsymbol{y}_1^T, \ldots, \boldsymbol{y}_n^T]^T$, respectively. A segment of a sequence is given by $x_{k-L}^k = [x_{k-L}, \ldots, x_k]^T$.

2. SYSTEM MODEL

The considered system model is based on the discrete time system model described before in [6]. Later in Section 4 the model is extended by different CPM demodulators for processing the quantized received signal, as illustrated in Fig. 1.

2.1. CPM Modulator

The information conveying phase term of a CPM signal [1] reads

$$\phi(t) = 2\pi h \sum_{k=0}^{\infty} \alpha_k f(t - kT_s) + \varphi_0, \tag{1}$$

where T_s denotes the symbol duration, $h = \frac{K_{cpm}}{P_{cpm}}$ is the modulation index, $f(\cdot)$ is the phase response, φ_0 is a phase-offset and α_k represents the kth transmit symbol. For an even modulation order M_{cpm}, such transmit symbols are taken from an alphabet described by $\alpha_k \in \{\pm 1, \pm 3, \ldots, \pm(M_{cpm} - 1)\}$. In order to obtain a finite number of phase states K_{cpm} and P_{cpm} must be relative prime positive integers. The phase response function $f(\cdot)$ shapes the sequence of CPM symbols to the continuous phase signal with smooth transitions. The phase response is characterized by

$$f(\tau) = \begin{cases} 0, & \text{if } \tau \le 0, \\ \frac{1}{2}, & \text{if } \tau > T_{cpm}, \end{cases}$$

where T_{cpm} defines the CPM memory in terms of $L_{cpm} = \lceil T_{cpm}/T_s \rceil$ transmit symbols. In general, the corresponding phase trellis of (1) is time variant, which means that the possible phase states are time-dependent. A time invariant trellis can be constructed by tilting the
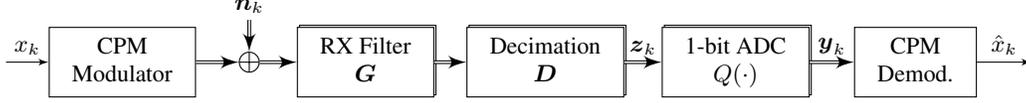
Fig. 1: Discrete time description of the CPM system with 1-bit quantization and oversampling at the receiver
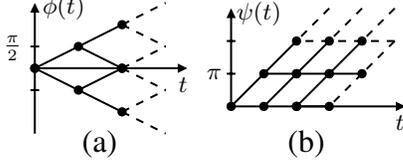
Fig. 2: CPM trellis (a) and its tilted version (b), $M_{\text{cpm}} = 2$, $h = 1/2$, $\phi_0 = 0$, $L_{\text{cpm}} = 1$ and linear phase transition

phase according to the decomposition approach in [10]. The tilt corresponds to a frequency offset applied to the CPM signal, i.e., the phase term becomes $\psi(t) = \phi(t) + 2\pi\Delta ft$, where $\Delta f = h(M_{\text{cpm}}-1)/2T_{\text{s}}$. In this context, Fig. 2 shows the tilted version of a MSK signal. Taking into account the tilted trellis, a different symbol notation $x_k = (\alpha_k + M_{\text{cpm}} - 1)/2$ can be considered, which then corresponds to the symbol alphabet $\mathcal{X} = \{0, 1, \ldots, M_{\text{cpm}} - 1\}$. The tilted CPM phase $\psi(t)$ within one symbol interval with duration T_{s}, letting $t = \tau + kT_{\text{s}}$, is fully described by the state definition $\tilde{s}_k = \left[\beta_{k-L_{\text{cpm}}}, x_{k-L_{\text{cpm}}+1}^k\right]$ in terms of

$$\psi(\tau + kT_{\text{s}}) = \frac{2\pi}{P_{\text{cpm}}}\beta_{k-L_{\text{cpm}}} \tag{2}$$
$$+ 2\pi h \sum_{l=0}^{L_{\text{cpm}}-1} (2x_{k-l} - M_{\text{cpm}} + 1) f(\tau + lT_{\text{s}})$$
$$+ \pi h (M_{\text{cpm}} - 1) \left(\frac{\tau}{T_{\text{s}}} + L_{\text{cpm}} - 1\right) + \varphi_0,$$

where the absolute phase state $\beta_{k-L_{\text{cpm}}}$ can be reduced to

$$\beta_{k-L_{\text{cpm}}} = \left(K_{\text{cpm}} \sum_{l=0}^{k-L_{\text{cpm}}} x_l\right) \bmod P_{\text{cpm}},$$

which is related to the 2π-wrapped accumulated phase contributions of the input symbols that are prior to the CPM memory.

In the sequel a discrete time description is considered which implies that the CPM phase is represented in a vector notation. The corresponding tilted CPM phase $\psi(\tau + kT_{\text{s}})$ for one symbol interval, i.e., $0 \leq \tau < T_{\text{s}}$, is then discretized into MD samples, which composes the vector denoted by $\boldsymbol{\psi}_k(\tilde{s}_k) = [\psi(\frac{T_{\text{s}}}{MD}(kMD+1)), \psi(\frac{T_{\text{s}}}{MD}(kMD+2)), \ldots, \psi(T_{\text{s}}(k+1))]^T$, where M is the oversampling factor, and D is a higher resolution multiplier. The tilt of the phase can be established in the actual communication system by receiving at an intermediate frequency (IF). With this, we can consider that different low-IF frequencies can be used, which motivates the definition of $\psi_{\text{IF}}(t) = \psi(t) + 2\pi\frac{n_{\text{IF}}}{T_s}t$. Choosing $n_{\text{IF}} > 0$ is promising because the appearance of zero-crossings can be adjusted, as proposed in [7]. Nevertheless, in the considered examples $n_{\text{IF}} = 0$ is chosen for simplicity.

Regarding the discrete system model in Fig. 1, the CPM modulator takes the input sequence x^n and generates the transmit signal

$\sqrt{\frac{E_s}{T_s}}e^{j\boldsymbol{\psi}_k(\tilde{s}_k)}$, where E_s is the symbol energy, i.e., it already takes into account the frequency offset.

2.2. Receive filter and 1-bit quantization

The receive filter $g(t)$ has an impulse response of length T_g. In the discrete model for expressing a subsequence of $(\eta + 1)$ oversampling output symbols it is represented in a matrix form with $\boldsymbol{G}$, as a $MD(\eta + 1) \times MD(L_g + \eta + 1)$ Topeliz matrix, whose first row is $[\boldsymbol{g}^T, \boldsymbol{0}_{MD(\eta+1)}^T]$, where $\boldsymbol{g}^T = [g(L_g T_s), g(\frac{T_s}{MD}(L_g MD - 1)), \ldots, g(\frac{T_s}{MD})]$. A higher sampling grid in the waveform signal, in the noise generation and in the filtering is adopted to adequately model the aliasing effect. This receive filtering yields an increase of memory in the system by L_g symbols, where $(L_g - 1)T_s < T_g \leq L_g T_s$. This motivates the definition of the overall memory in terms of $L = L_{\text{cpm}} + L_g$.

The filtered samples are decimated to the vector $\boldsymbol{z}_{k-\eta}^k$ according to the oversampling factor M, by multiplication with the D-fold decimation matrix $\boldsymbol{D}$, as described in equation (16) in [6], with dimensions $M(\eta + 1) \times MD(\eta + 1)$. Then, the result $\boldsymbol{z}_{k-\eta}^k$ is 1-bit quantized to the vector $\boldsymbol{y}_{k-\eta}^k$. These operations can be represented by the following equations

$$\boldsymbol{y}_{k-\eta}^k = Q\left(\boldsymbol{z}_{k-\eta}^k\right) = Q\left(\boldsymbol{D}\,\boldsymbol{G}\left[\sqrt{\frac{E_s}{T_s}}e^{\boldsymbol{\psi}_{k-\eta-L_g}^k} + \boldsymbol{n}_{k-\eta-L_g}^k\right]\right), \tag{3}$$

where the quantization operator $Q(\cdot)$ is applied element-wise. The quantization of $\boldsymbol{z}_k$ is described by $y_{k,m} = \text{sgn}(\text{Re}\{z_{k,m}\}) + j\text{sgn}(\text{Im}\{z_{k,m}\})$, where m denotes the oversampling index which runs from 1 to M. The vector $\boldsymbol{n}_{k-\eta-L_g}^k$ contains complex zero-mean white Gaussian noise samples with variance $\sigma_n^2 = N_0$.

3. PROPOSED FASTER-THAN-NYQUIST CPM

As known from linear modulation schemes, a faster-than-Nyquist signaling can yield a benefit for the design of zero-crossings [11], which is key for channels with 1-bit quantization at the receiver. In this section, a new subclass of CPM waveforms is introduced which provides relatively high, signaling rate and high spectral efficiency at the same time. Illustrated configurations of the proposed waveform only require low-complexity at the transmitter and receiver.

In the sequel the proposed waveform is considered with the rectangular frequency pulse with duration T_{cpm}, but the extension to pulses like raised cosine and Gaussian pulse is possible.

3.1. Proof-of-concept of Faster-than-Nyquist CPM

In this section, it is shown that CPM signals can be constructed with significantly reduced symbol duration as compared to standard CPFSK, which convey the same information per time interval and occupy the same bandwidth. Because of its mathematical tractability, Carson's bandwidth criterion, as used in [12, 13], is considered
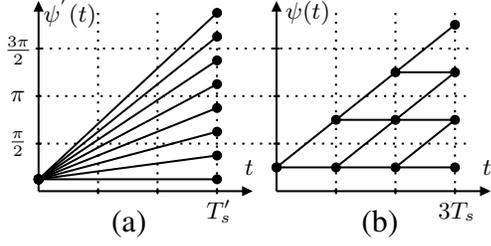
Fig. 3: 8-symbol CPFSK (a) and three-symbol-period FTN-CPM (b) tilted trellises

Fig. 5: Tilted CPM constellation diagram (a) and trellis (b) of the proposed FTN-CPM with $T_{\mathrm{cpm}} = T_{\mathrm{s}}$, $h = 1/4$ and $\phi_0 = \pi/4$

Fig. 4: Equi-bandwidth $(B_{\mathrm{c}}/B_{\mathrm{c}}')$ lines, $T_{\mathrm{s}}'/T_{\mathrm{s}} = 3$, $M_{\mathrm{cpm}} = 2$

in this section. Following the steps in [12], the bandwidth for CPM signals with i.u.d. input and rectangular frequency pulse reads as

$$B_{\mathrm{c}} = h\sqrt{(M_{\mathrm{cpm}}^2 - 1)(3T_{\mathrm{s}}T_{\mathrm{cpm}})^{-1} + T_{\mathrm{cpm}}^{-1}}. \qquad (4)$$

As a reference, a standard CPFSK signal shall be considered, whose parameters are indicated with $'$. The reference CPFSK is fully described by T_{s}', M_{cpm}', $h' = \frac{1}{M_{\mathrm{cpm}}'}$, $T_{\mathrm{cpm}}' = T_{\mathrm{s}}'$ and B_{c}'. Now, it is aimed to construct a FTN-CPM signal with a shorter symbol duration T_{s}, such that the ratio $T_{\mathrm{s}}'/T_{\mathrm{s}}$ is an integer value, as shown in Fig. 3. The conveyed information per time interval is equal for both signals by defining $M_{\mathrm{cpm}}^{T_{\mathrm{s}}'/T_{\mathrm{s}}} = M_{\mathrm{cpm}}'$. With this, the relation between the bandwidth of the FTN-CPM signal and the reference CPFSK signal can be expressed as

$$\frac{B_{\mathrm{c}}}{B_{\mathrm{c}}'} = \frac{T_{\mathrm{s}}'}{T_{\mathrm{s}}} \left(h\sqrt{\frac{M_{\mathrm{cpm}}^2 - 1}{3T_{\mathrm{cpm}}/T_{\mathrm{s}}}} + \frac{T_{\mathrm{s}}}{T_{\mathrm{cpm}}} \right) \left(1 + \frac{1}{M_{\mathrm{cpm}}^{T_{\mathrm{s}}'/T_{\mathrm{s}}}} \sqrt{\frac{M_{\mathrm{cpm}}^{2T_{\mathrm{s}}'/T_{\mathrm{s}}} - 1}{3}} \right)^{-1}. \qquad (5)$$

For the case of predefined design parameter $(T_{\mathrm{s}}'/T_{\mathrm{s}})$ and M_{cpm}, the relation in (5) is a function of modulation index h and relative frequency pulse length $T_{\mathrm{cpm}}/T_{\mathrm{s}}$. Aiming for a high spectral efficiency for the FTN-CPM signal a low relative bandwidth (5) is promising. An example case is illustrated for $T_{\mathrm{s}}'/T_{\mathrm{s}} = 3$ and $M_{\mathrm{cpm}} = 2$. As can be seen, the bandwidth increase brought by the higher signaling rate can be compensated by adjustment of the modulation index h and the length of the frequency pulse T_{cpm}. In the sequel the FTN-CPM waveform configurations are detailed which are promising in the presence of 1-bit quantization at the receiver.

3.2. FTN-CPM for 1-bit quantization at the receiver

A widely used waveform design criterion for channels with 1-bit quantization at the receiver is given by the maximization of distance

to the decision threshold [14]. By assuming that the receive filter $g(t)$ only marginally changes the signal phase $\psi(t)$ at the receiver, zero-crossings appear whenever the phase crosses integer multiples of $\frac{\pi}{2}$. Considering that sampling rate is equal to the FTN signaling rate, the illustrated FTN-CPM phase tree on the RHS of Fig. 3 is optimal in terms of distance to decision threshold. The corresponding binary FTN-CPM constellation diagram is shown in Fig. 5, which implies that a zero-crossing conveys the transmit symbol 1 and 0 else. In order to achieve a spectral efficiency similar to the corresponding conventional CPFSK waveform, the length of the frequency pulse T_{cpm} can be increased, cf. Fig. 4, where different cases are examined in the sequel.

4. CPM DEMODULATION

This section describes two demodulation methods.

4.1. MAP Detection

The MAP decision metric for each symbol x_k is given by the A Posteriori Probability (APP) $P\left(x_k|\boldsymbol{y}^n\right)$. For the considered system, approximated APPs $P_{\mathrm{aux}}\left(x_k|\boldsymbol{y}^n\right)$ can be computed via a BCJR algorithm [15] that is based on an auxiliary channel law. Depending on the receive filter, noise samples are correlated which implies dependency on previous channel outputs, such that the channel law has the form $P(\boldsymbol{y}_k|\boldsymbol{y}^{k-1}, x^n)$. In this case the consideration of an auxiliary channel law $W(\cdot)$ is required [6], which can be described by

$$W(\boldsymbol{y}_k|\boldsymbol{y}^{k-1}, x^n) = P(\boldsymbol{y}_k|\boldsymbol{y}_{k-N}^{k-1}, \beta_{k-L-N}, x_{k-L-N+1}^k)$$
$$= \frac{P(\boldsymbol{y}_{k-N}^k|\beta_{k-L-N}, x_{k-L-N+1}^k)}{P(\boldsymbol{y}_{k-N}^{k-1}|\beta_{k-L-N}, x_{k-L-N+1}^{k-1})}, \qquad (6)$$

where the dependency on N previous channel outputs is taken into account. With this, an extended state representation is required which is denoted by

$$s_k = \begin{cases} [\beta_{k-L-N+1}, x_{k-L-N+2}^k], & \text{if } L + N > 1, \\ [\beta_k], & \text{if } L + N = 1, \end{cases} \qquad (7)$$

where $L + N$ is the total memory of the system. Based on the state notation in (7) the probabilities for the channel law (6) can be cast as $P\left(\boldsymbol{y}_{k-N}^k|s_k, s_{k-1}\right)$ and $P\left(\boldsymbol{y}_{k-N}^{k-1}|s_{k-1}\right)$. Its computation involve a multivariate Gaussian integration in terms of

$$P\left(\boldsymbol{y}_{k-N}^k|s_k, s_{k-1}\right) = \int\limits_{\boldsymbol{z}_{k-N}^k \in \mathbb{Y}_{k-N}^k} p(\boldsymbol{z}_{k-N}^k|s_k, s_{k-1})d\boldsymbol{z}_{k-N}^k, \qquad (8)$$
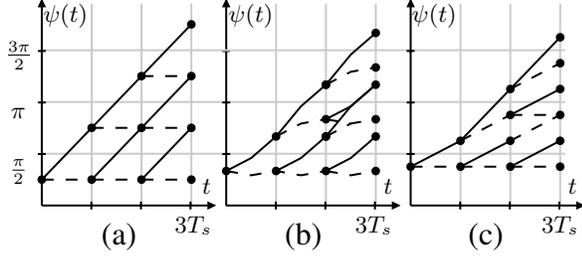
Fig. 6: Simple receive strategy: decide for 0 (dashed line) and 1 (solid line); Different FTN-CPM configurations: (a) $T_{\mathrm{cpm}} = T_{\mathrm{s}}$, (b) $T_{\mathrm{cpm}} = 1.5T_{\mathrm{s}}$ and (c) $T_{\mathrm{cpm}} = 2T_{\mathrm{s}}$

where $\boldsymbol{z}_{k-N}^k$ is a complex Gaussian random vector that describes the input of the ADC, with a mean vector defined by $\boldsymbol{\mu}_x = \boldsymbol{D}\,\boldsymbol{G}\left[\sqrt{\frac{E_{\mathrm{s}}}{T_{\mathrm{s}}}}e^{\psi_{k-N-L_g}^k}\right]$, and covariance matrix $\boldsymbol{R} = \sigma_n^2\boldsymbol{D}\boldsymbol{G}\boldsymbol{G}^H\boldsymbol{D}^T$, with $\boldsymbol{D}$ and $\boldsymbol{G}$ as introduced before with $\eta = N$. The integration interval is expressed in terms of the quantization region $\mathbb{Y}_{k-N}^k$ that belongs to the channel output symbol $\boldsymbol{y}_{k-N}^k$. After rewriting (8) as a real valued multivariate Gaussian integration, how it is done in equation (21) in [6], the algorithm in [16] can be applied. Finally the BCJR algorithm provides the probabilities $P_{\mathrm{aux}}\left(s_{k-1}, s_k | \boldsymbol{y}^n\right)$ which are subsequently used for computing the symbol APPs via $P_{\mathrm{aux}}\left(x_k | \boldsymbol{y}^n\right) = \sum_{\forall s_{k-1}, s_k \supseteq x_k} P_{\mathrm{aux}}\left(s_{k-1}, s_k | \boldsymbol{y}^n\right)$. The multivariate Gaussian integration (8) becomes computationally expensive when M, M_{cpm} and the channel memory are high, as detailed in [7]. Note that for uncorrelated noise samples, subsequent channel outputs are independent, such that $P(\boldsymbol{y}_k | \boldsymbol{y}^{k-1}, x^n) = P(\boldsymbol{y}_k | x^n)$, obviating the need for an auxiliary channel law.

4.2. The Proposed Simple Demodulator

In order to relieve the computational load at the receiver, some versions of the proposed FTN-CPM scheme can be demodulated with an alternative simple strategy. The receive strategy for the binary FTN-CPM case with $h = \frac{1}{4}$, and sufficiently small T_{cpm}, like $T_{\mathrm{cpm}} = 2T_{\mathrm{s}}$, only involves the evaluation of a change in real or imaginary part, depending on the previous sample y_{k-1}, which can be cast as

$$\hat{x}_k = \begin{cases} \frac{1}{2}|\{\mathrm{Re}\{y_k\} - \mathrm{Re}\{y_{k-1}\}|, & \text{if } y_{k-1} \in \{1+j, -1-j\}, \\ \frac{1}{2}|\{\mathrm{Im}\{y_k\} - \mathrm{Im}\{y_{k-1}\}|, & \text{if } y_{k-1} \in \{1-j, -1+j\}. \end{cases}$$

Fig. 6 illustrates the receiver decisions in a noise-free scenario for $T_{\mathrm{cpm}} = T_{\mathrm{s}}$ in Fig. 6(a), $T_{\mathrm{cpm}} = 1.5T_{\mathrm{s}}$ in Fig. 6(b) and $T_{\mathrm{cpm}} = 2T_{\mathrm{s}}$ in Fig. 6(c), where the phase distortion brought by the receive filter is neglected for illustration purpose. Note that for larger values for T_{cpm} the noise sensitivity increases. A special case is given by $T_{\mathrm{cpm}} = 2T_{\mathrm{s}}$ which results in the same number of equidistant constellation points as the corresponding 8-symbol CPFSK.

5. NUMERICAL RESULTS

In order to preserve the transmit waveform and its zero-crossings, a suboptimal short bandpass receive filter is considered as follows

$$g(t) = \sqrt{\frac{1}{T_g}}\mathrm{rect}\left(\frac{t - T_g/2}{T_g}\right) \cdot e^{j2\pi\Delta f(t - T_g/2)}, \qquad (9)$$

which is similar to the integrate and dump receiver considered in [17]. Note that the common receiver based on a matched filter

bank is hardware demanding and not compatible with the considered 1-bit approach. Table 1 gathers the simulation parameters for all considered CPM waveforms. 4-CPFSK [6] serves a standard reference waveform, which provides reliable communication without additional coding when considering 1-bit quantization. The same holds for 8-CPFSK [7] which serves as reference waveform that does not require additional coding for $M = 5$ and optimized low-IF with $n_{\mathrm{IF}} = 0.25$. The proposed FTN-CPM is represented by the running example from Section 3 and 4 specified by $M_{\mathrm{cpm}} = 2$, $h = \frac{1}{4}$ and rectangular frequency pulse with different durations T_{cpm}. Note that for the considered FTN-CPM schemes the receive filter is such that noise samples are uncorrelated and an auxiliary channel law (specified by N) is not required.

Waveform	Simulation Parameters
4-CPFSK [6]	$M_{\mathrm{cpm}} = 4, L_{\mathrm{cpm}} = 1, T_g = 0.5T_{\mathrm{s}},$ $h = 1/4, n_{\mathrm{IF}} = 0, \phi_0 = \pi/4, N = 0$
8-CPFSK [7]	$M_{\mathrm{cpm}} = 8, L_{\mathrm{cpm}} = 1, M = 5, T_g = 0.5T_{\mathrm{s}},$ $h = 1/8, n_{\mathrm{IF}} = 0.25, \phi_0 = \pi/8, N = 0$
Proposed FTN-CPM	$M_{\mathrm{cpm}} = 2, M = 1, T_g = T_{\mathrm{s}},$ $h = 1/4, n_{\mathrm{IF}} = 0, \phi_0 = \pi/4$

Table 1: Considered waveforms

The adjustable power containment bandwidth is considered, where we refer to 90% power containment ($B_{90\%}$) as default and use for some cases also 95%. The considered SNR is defined by

$$\mathrm{SNR} = \frac{\lim_{T \to \infty}\frac{1}{T}\int_T |x(t)|^2\,dt}{N_0\,B_{90\%}} = \frac{E_{\mathrm{s}}}{N_0}(T_{\mathrm{s}}B_{90\%})^{-1}, \quad (10)$$

where $x(t) = \sqrt{\frac{E_{\mathrm{s}}}{T_{\mathrm{s}}}}e^{j\psi(t)}$ is the complex low-IF representation of the signal and the noise power density N_0 corresponds to the variance of the noise samples in (3).

5.1. Spectral Efficiency and Effective Oversampling Ratio

The spectral efficiency w.r.t. $B_{90\%}$ reads

$$\text{spectral eff.} = \frac{I_{\mathrm{bpcu}}}{B_{90\%}T_{\mathrm{s}}} \text{ [bit/s/Hz]}, \qquad (11)$$

where I_{bpcu} is the achievable rate w.r.t. one symbol duration T_{s}, which is computed by applying the methods developed in [6]. The effective oversampling ratio w.r.t. $B_{90\%}$ is given by $\mathrm{OSR}' = M\,(B_{90\%}T_{\mathrm{s}})^{-1}$. Table 2 displays computed values for effective oversampling factor and maximum spectral efficiency for the waveforms considered in Table 1. Moreover, Fig. 7 illustrates the spectrum efficiency w.r.t. $B_{90\%}$ versus SNR. It is shown that choosing $T_{\mathrm{cpm}} \geq 1.6T_{\mathrm{s}}$ yields a higher spectral efficiency as the corresponding CPFSK waveform for medium and high SNR. When referring to the $B_{95\%}$ it is required to choose $T_{\mathrm{cpm}} \geq 2T_{\mathrm{s}}$ for approaching the spectral efficiency of the corresponding CPFSK, cf. Table 2.

Waveform	$\frac{T_{\mathrm{cpm}}}{T_{\mathrm{s}}}$	M	$\frac{\log_2 M_{\mathrm{cpm}}}{B_{90\%}T_{\mathrm{s}}}$	$\frac{\log_2 M_{\mathrm{cpm}}}{B_{95\%}T_{\mathrm{s}}}$	OSR'
8-CPFSK [7]	1	5	**3.467**	**2.873**	5.778
4-CPFSK [6]	1	4	2.372	1.976	4.744
4-CPFSK [6]	1	2	2.372	1.976	2.372
Proposed FTN-CPM	1	1	2.853	1.983	2.853
Proposed FTN-CPM	1.6	1	**3.507**	2.544	3.507
Proposed FTN-CPM	2	1	3.891	**2.881**	3.891

Table 2: Bandwidths and effective oversampling factor
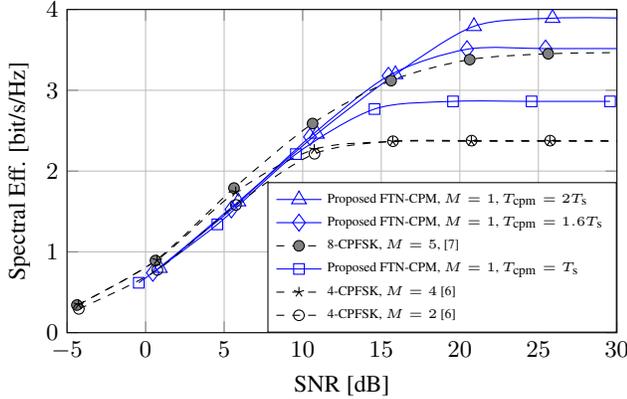
Fig. 7: Spectral Efficiency with respect to the 90% power containment bandwidth
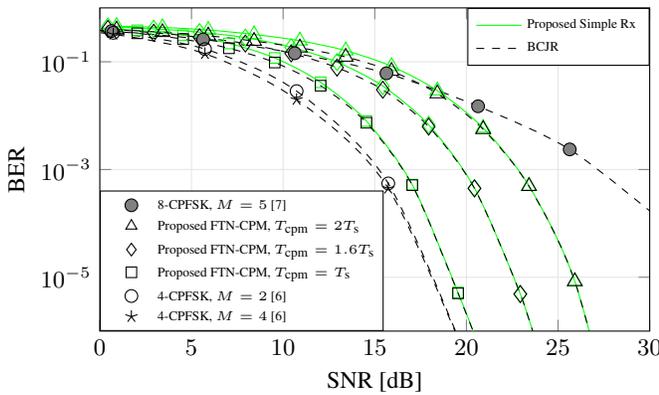
Fig. 8: BER performance of the considered CPM waveforms

5.2. Bit Error Rate

The uncoded BER is shown in Fig. 8. The increase of the length of the frequency pulse T_{cpm} in the proposed binary CPM reduces the distance between the constellations points, which results in increased sensitivity to noise. Different to the 1-bit customized 8-CPFSK [7], the proposed FTN-CPM shows a BER performance which decreases fast for higher SNR. An additional highlight is that the proposed simple receiver strategy results in a BER performance which is almost identical with the performance of the optimal BCJR-based CPM demodulator especial at medium and high SNR.

6. CONCLUSIONS

The present study introduces a novel subclass of CPM signals, namely CPM signals with *faster-than-Nyquist* signaling. The novel waveform is especially promising in the context of 1-bit quantization at the receiver, because it provides a good steering of zero-crossings. By considering Carson's bandwidth criterion it is shown that a waveform equivalent to common CPFSK in bandwidth and information bits can be constructed with a higher signaling rate. Numerical results show superior performance in terms of spectral efficiency and BER for the channel with 1-bit quantization at the receiver. The illustrated binary FTN-CPM signal can be detected with an extremely simple detector with a performance close to MAP detection.

7. REFERENCES

[1] J. Anderson, T. Aulin, and C. E. Sundberg, *Digital Phase Modulation*, Plenum Press, New York, 1986.

[2] C. E. Sundberg, "Continuous phase modulation," *IEEE Commun. Mag.*, vol. 24, no. 4, pp. 25–38, April 1986.

[3] R.H. Walden, "Analog-to-digital converter survey and analysis," *IEEE J. Sel. Areas Commun.*, vol. 17, no. 4, pp. 539 –550, Apr. 1999.

[4] S. Shamai (Shitz), "Information rates by oversampling the sign of a bandlimited process," *IEEE Trans. Inf. Theory*, vol. 40, no. 4, pp. 1230–1236, July 1994.

[5] L. Landau, M. Dörpinghaus, and G. Fettweis, "1-bit quantization and oversampling at the receiver: Communication over bandlimited channels with noise," *IEEE Commun. Lett.*, vol. 21, no. 5, pp. 1007–1010, May 2017.

[6] L. T. N. Landau, M. Dörpinghaus, R. C. de Lamare, and G. P. Fettweis, "Achievable rate with 1-bit quantization and oversampling using continuous phase modulation-based sequences," *IEEE Trans. Wireless Commun.*, vol. 17, no. 10, pp. 7080–7095, Oct 2018.

[7] S. Bender, M. Dörpinghaus, and G. P. Fettweis, "The potential of continuous phase modulation for oversampled 1-bit quantized channels," in *in Proc. IEEE Int. Workshop Signal Process. Adv. Wireless Commun.*, Cannes, France, July 2019.

[8] R. R. M. de Alencar, L. T. N. Landau, and R. C. de Lamare, "Continuous phase modulation with 1-bit quantization and oversampling using soft detection and iterative decoding," in *in Proc. of the Asilomar Conference on Signals, Systems, and Computers*, Pacific Grove, CA, USA, Oct 2019.

[9] J. E. Mazo, "Faster-than-Nyquist signaling," *Bell System Technical Journal*, vol. 54, no. 1, pp. 1451–1462, Oct. 1975.

[10] B. E. Rimoldi, "A decomposition approach to CPM," *IEEE Trans. Inf. Theory*, vol. 34, no. 2, pp. 260–270, Mar. 1988.

[11] L. T. N. Landau, M. Dörpinghaus, and G. P. Fettweis, "1-bit quantization and oversampling at the receiver: Sequence-based communication," *EURASIP J. Wireless Commun. Netw.*, vol. 17, no. 83, 2018.

[12] C. H. Kuo and K. M. Chugg, "On the bandwidth efficiency of CPM signals," in *Proc. IEEE Military Com. Conf. (MILCOM)*, Monterey, CA, USA, Oct 2004, vol. 1, pp. 218–224.

[13] A. Barbieri, A. Cero, A. Piemontese, and G. Colavolpe, "Markov capacity of continuous phase modulations," in *Proc. IEEE Int. Symp. Inform. Theory (ISIT)*, Nice, France, June 2007, pp. 161–165.

[14] L. Landau, S. Krone, and G. P. Fettweis, "Intersymbol-interference design for maximum information rates with 1-bit quantization and oversampling at the receiver," in *Proc. of the International ITG Conference on Systems, Communications and Coding*, Munich, Germany, Jan. 2013.

[15] L. Bahl, J. Cocke, F. Jelinek, and J. Raviv, "Optimal decoding of linear codes for minimizing symbol error rate (corresp.)," *IEEE Trans. Inf. Theory*, vol. 20, no. 2, pp. 284–287, Mar. 1974.

[16] A. Genz, "Numerical computation of multivariate normal probabilities," *J. Comput. Graph. Stat.*, pp. 141–149, 1992.

[17] M. H. M. Costa, "A practical demodulator for continuous phase modulation," in *Proc. IEEE Int. Symp. Inform. Theory (ISIT)*, Trondheim, Norway, Jun 1994, p. 88.